DALTON
FULL PAPER

Electron localisation in electrochemically reduced mono- and bi-nuclear rhenium(I) complexes with bridged polypyridyl ligands †

Simon E. Page, Amar Flood and Keith C. Gordon *

Department of Chemistry, Union Place, University of Otago, Dunedin, New Zealand.
E-mail: kgordon@alkali.otago.ac.nz

Received 22nd November 2001, Accepted 29th January 2002
First published as an Advance Article on the web 19th February 2002

A number of mono- and bi-nuclear rhenium(I) complexes have been prepared and their physical properties, including the infrared spectra of the reduced complexes, have been studied. These compounds have the general formula $[Re(CO)_3Cl(L)]$ and $[Cl(CO)_3Re(\mu\text{-}L)Re(CO)_3Cl]$, where L can be 2,3-(2′,2″)-diquinolylquinoxaline, 6,7-dimethyl-2,3-(2′,2″)-diquinolylquinoxaline, 2,3-(2′,2″)-diquinolylbenzoquinoxaline, 6,7-dichloro-2,3-(2′,2″)-diquinolylquinoxaline, 2,3-(2′,2″)-diquinoxalylquinoxaline, 6,7-dimethyl-2,3-(2′,2″)-diquinoxalylquinoxaline, 2,3-(2′,2″)-diquinoxalylbenzoquinoxaline and 6,7-dichloro-2,3-(2′,2″)-diquinoxalylquinoxaline. The electrochemical studies show that the first reduction potential of the free ligands correlates with the reductions of the corresponding mono- and bi-nuclear complexes. The properties of the complexes have been modelled using semi-empirical methods. These show linear correlations between: (a) the energy of the MLCT transitions versus the difference in energy between the LUMO and the HOMO and (b) the change in carbonyl force constant with reduction *vs.* the wavefunction amplitude of the π* LUMO at the site of coordination. The experimental data and calculations point to significant alterations in the π* LUMO with substitution at the ligand and with the chelation of a second Re(I) center.

Introduction

Metal polypyridyl complexes have been widely studied, in part, because of their potential utility in photocatalysis,[1] including CO_2 remediation,[2] solar energy systems[3] and molecular electronics,[4] including light-emitting diodes.[5] In almost all of these complexes the key excited state is MLCT in nature.[1–3]

One way to model part of the excited state is to electrochemically reduce the complex and establish the nature of the MO populated by the reducing electron,[6–11] the so-called redox MO.[12] The properties of metal complexes, with respect to MLCT photo-excitation and in electron transfer schemes will be mitigated and controlled by the nature of the redox MO.[13]

We have studied a series of mono- and bi-nuclear rhenium(I) complexes with a variety of bridging ligands in an attempt to understand how coordination of a 2° metal and substitution at the ligand alter the nature of the redox MO. Complexes with $\{Re(CO)_3Cl\}$ moieties tend to interact strongly with bridging ligands and this can lead to unexpected polarisation of the redox MO.[14]

The ligands used, depicted in Fig. 1, may be considered as having arms (quinoline or quinoxaline, labelled 1′–8′ and 1″–8″ in Fig. 1) and a bridge (quinoxaline, labelled 1–8, Fig. 1). The bridging ligands fall into two classes, diquinoline–quinoxaline (dqq, **1**–**4**) and diquinoxaline–quinoxaline (dqxq, **5**–**8**).

We have utilised simple semi-empirical calculations in order to assist data interpretation.

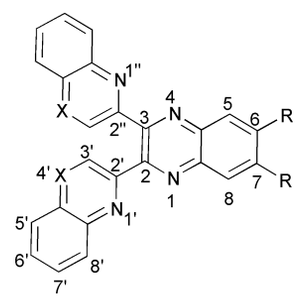

Fig. 1 Ligands used in this study, with numbering scheme for NMR data. Ligands are labelled: **1** (R = H, X = CH); **2** (R = CH_3, X = CH); **3** (R = benzo, X = CH); **4** (R = Cl, X = CH); **5** (R = H, X = N); **6** (R = CH_3, X = N); **7** (R = benzo, X = N); **8** (R = Cl, X = N).

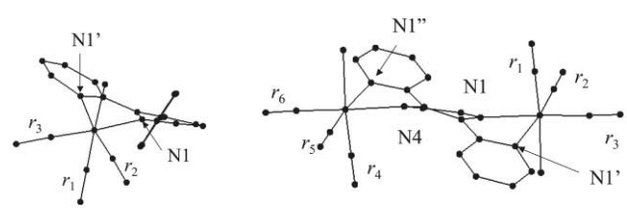

Fig. 2 Calculated structures for Re**1** and Re_2**1**. For clarity only the bonding rings are shown and H atoms have been removed. The internal coordinates for CO vibrations are also shown (r_1 through r_6) with the numbering scheme for the bonding N atoms.

Results and discussion

The structure of each of the complexes was optimised using semi-empirical calculations with PM3 parameterization. Representative examples are shown in Fig. 2. The calculations show that the mononuclear complexes with quinoline and quinoxaline armed ligands have the unbound arm almost perpendicular to the bound ring systems. The bound ring systems are distorted, bowing in an arc and displaying a 26° dihedral angle with respect to the Re–N linkage and the bridging C–C bond (Fig. 1, C2, C2′) of the ligand. No crystallographic data are available for the complexes reported herein but a structure is available for the related $[Re(CO)_3(dpq)Cl]$ complex.[15] This also reveals the bowing of the bound ligand rings to the Re–N bond (*ca.* 23°). A PM3 calculation of

† Electronic supplementary information (ESI) available: force constants of the mono- and bi-nuclear $[Re(CO)_3Cl]$ complexes of **1**–**8** in CH_2Cl_2 solution. See http://www.rsc.org/suppdata/dt/b1/b110730p/

 DOI: 10.1039/b110730p

$[Re(CO)_3(dpq)Cl]$ overestimates the angle between the unbound pyridine ring and the bound quinoxaline; it is probable this overestimation also occurs in the dqq and dqxq complexes.

The calculated structure of the binuclear complexes are similar. Re_2**1** (Fig. 2) shows a twisting of the bridging ligand with a dihedral angle of 42° between the two arms of the ligand (Fig.1, C2′, C2, C3, C2″). The bound rings at each chelating site show a bowed structure similar to that observed in the mononuclear complex.

The binuclear complexes produced have the ability to form as isomers, with the Cl groups *cis* or *trans* to one another. This has been observed and commented on by Kaim *et al.*[16] and Lehn *et al.*[17] in previous studies. These studies suggest that there is little difference in terms of electronic properties between the two isomers. This is in contrast to recent work on $\{Ru(bpy)_2\}^{2+}$ binuclear complexes which can show significant differences with diastereoisomers.[18] In this work a substantial part of the isomer effect is attributed to ion-pairing which would not occur with the neutral complexes described herein.

The PM3 calculations provide a vibrational output and this may be used to give some insight into which of the binuclear complexes' isomers are present. The PM3 predictions for ν(CO) are generally between 1–3% too high but the observed relative pattern, one high wavenumber band and two lower wavenumber bands, is predicted for the mononuclear complexes. The lack of absolute accuracy in the frequencies calculated is unsurprising in view of the fact that semi-empirical calculations use restricted basis sets and neglect atomic orbital overlap between adjacent nuclei.[19] The parameters used for PM3 calculations have been optimised to reproduce reliable equilibrium geometries,[20] but recently PM3 calculations have been utilised to provide insight into vibrational and electronic spectral properties.[21] In the case of the binuclear complexes structures may be optimised in *cis* or *trans* configurations, with respect to Cl atoms. The IR frequencies predicted for each isomer have the following features; for the *trans*-Cl isomer a 10 cm^{-1} splitting is predicted for the high wavenumber mode, the lower wavenumber modes also show splitting but of only a few wavenumbers. All of the IR data are given in Table 4 (see later). The *cis*-isomer[22] also shows a 10 cm^{-1} splitting of the high wavenumber mode, but additionally one of the lower wavenumber modes is predicted to split by 12 cm^{-1}. The experimental data on these systems does not show *cis*-isomer behaviour and this suggests the bulk of the samples studied herein are in a *trans* configuration.

Molecular orbital energies

The electronic absorption and electrochemical data provide experimental probes of the energetics of the dπ and ligand π* MOs. The electrochemical data (Table 1) show that the substitution of an electron-withdrawing group, such as chloro- or benzo-, makes the ligand easier to reduce by *ca.* 100 mV. Furthermore, the substitution of quinoline arms for quinoxaline also results in easier reduction, *i.e.* the π* acceptor redox MO is stabilised, by *ca.* 100–200 mV. Arm substitution affects the $E^{0\prime}$ for reduction, this suggests that the three-ring systems of the ligands have some level of communication and are not orthogonal to each other. Note, the three-ring systems cannot be co-planar due to steric interactions between the 3′ and 3″ protons. The crystal structure of a related copper complex $[(PPh_3)_2Cu(\mu\text{-}\mathbf{4})Cu(PPh_3)_2](BF_4)_2$ has a torsion angle between the bridge and the arms of *ca.* 30°.[23]

The binding of $\{Re(CO)_3Cl\}$ to the ligands to form the respective mononuclear complexes significantly alters the electrochemistry. The $E^{0\prime}$ (1st reduction) is stabilised by 700–800 mV ($\Delta E^{0\prime}$). This may be compared to the dpq ligand which is stabilised by 800 mV on chelation to $\{Re(CO)_3Cl\}$.[24] Addition of a second $\{Re(CO)_3Cl\}$ unit further stabilises the $E^{0\prime}$ by *ca.* 300 mV. These data suggest that the nature of the LUMO on going from dqq to dqxq type ligands and mono- to bi-nuclear Re complexes changes. Calculations on the complexes can provide MO plots that can be related to these findings. The behaviour of each LUMO may be parameterised by c_N^2, this is the square of the wavefunction at each of the chelating N-atom sites.[25] These parameters are presented in Table 2.

Table 1 Electrochemical reduction potentials for **1**–**8** and their $\{Re(CO)_3Cl\}$ complexes in CH_2Cl_2 (1 mM where possible) with 0.1 M TBAP as supporting electrolyte. A Ag/AgCl reference electrode was used with ferrocene (+0.4 V *vs.* NHE) added as an internal standard. $E^{0\prime}$ was measured as the average position between the cathodic and anodic peak; this was estimated in the cases with limited reversibility

	$E^{0\prime}$/V (*vs.* NHE)	
1[a]	−1.54	
2[a]	−1.64[b]	
3	−1.29	
4[a]	−1.37	
5	−1.35	
6	−1.42	
7	−1.14	
8	−1.20	
Re**1**	−0.73	
Re**2**	−0.82	
Re**3**	−0.59	
Re**4**	−0.59	
Re**5**	−0.36	
Re**6**	−0.46	
Re**7**	−0.24	
Re**8**	−0.21	
Re_2**1**	−0.50	−1.25[c]
Re_2**2**	−0.57	
Re_2**3**	−0.40	−1.04
Re_2**4**	−0.37	−1.11[b]
Re_2**5**	−0.14	−0.71[b]
Re_2**6**	−0.23	−0.74[b]
Re_2**7**	−0.09	−0.70[b]
Re_2**8**	−0.07	−0.72[b]

[a] Previously published results. See ref. 18. [b] Indicates quasi-reversible electrode behaviour. [c] Indicates irreversible electrode behaviour.

The c_N^2 parameters show that the mononuclear dqq-type complexes, Re**1**–Re**4** have asymmetric LUMOs in which the greater proportion of the MO resides at the quinoxaline ring. On arm substitution to the dqxq complexes the value of c_N^2 for each of the chelating N atoms is closer (*i.e.* the LUMO is less asymmetric). In both cases the unbound ring shows no π* MO wavefunction amplitude. A more dramatic effect is evident for the c_N^2 of the binuclear complexes. These show large amplitude at the bridged ring system but almost none on the arms of the ligands.

The UV–Vis data shows absorptions due to ligand-based π–π* transitions and MLCT transitions (Table 3). MLCT transitions correlate with the energetics of the oxidation of the metal and reduction of the ligand. A plot of ν_{MLCT} *vs.* $E^{0\prime}$ (1st reduction), for complexes with a homologous series of ligands, should appear linear.[26,27] The ν_{MLCT} *vs.* $E^{0\prime}$ (1st reduction) parameters for the complexes may be fitted by the linear relationship, $\nu_{MLCT} = 0.7625E^{0\prime}$(1st reduction) + 2.1539 (R^2 = 0.97) for the mononuclear complexes, and by $\nu_{MLCT} = 0.5685E^{0\prime}$(1st reduction) + 1.812 (R^2 = 0.95) for the binuclear complexes. The linearity of these plots suggest the lowest MLCT transition is occupying the lowest π* MO on the ligand and that the Re dπ energies are reasonably invariant through the series of complexes.

The energy of the observed MLCT transition, $E_{MLCT,\ obsd}$ (eV), may be related to a calculated parameter, namely E(LUMO) − E(HOMO) ($E_{MLCT,\ calc}$). The absolute values of $E_{MLCT,\ calc}$ are much higher than the observed values, *ca.* 5 eV and the absolute values are clearly inaccurate; however a plot of $E_{MLCT,\ obs}$ *vs.* $E_{MLCT,\ calcd}$ is linear with $E_{MLCT,\ obs} = 1.44E_{MLCT,\ calcd}$ − 5.77 (R^2 = 0.98), suggesting that the calculations are

Table 2 Squared MO coefficients c_N^2 at the coordinating N centres (labelling from Fig. 1) for the LUMO, the predicted energies of HOMO and LUMO and the observed MLCT transition energies

	c_N^2					Energy/eV		
Complex	4	1′	1″	1	Σc_N^2	HOMO	LUMO	MLCT obsd.
Re**1**		0.140		0.197	0.337	−8.50	−2.64	2.71
Re**2**		0.136		0.199	0.335	−8.46	−2.58	2.77
Re**3**		0.125		0.207	0.332	−8.48	−2.66	2.67
Re**4**		0.130		0.199	0.329	−8.54	−2.75	2.58
Re**5**		0.166		0.172	0.338	−8.52	−2.74	2.51
Re**6**		0.168		0.168	0.336	−8.48	−2.68	2.60
Re**7**		0.153		0.186	0.339	−8.51	−2.76	2.46
Re**8**		0.156		0.177	0.333	−8.56	−2.84	2.44
Re_2**1**	0.217	0.032	0.032	0.217	0.499	−8.78	−3.41	2.02
Re_2**2**	0.216	0.032	0.032	0.216	0.497	−8.74	−3.32	2.07
Re_2**3**	0.198	0.034	0.034	0.197	0.463	−8.72	−3.39	1.93
Re_2**4**	0.215	0.030	0.030	0.215	0.490	−8.79	−3.48	1.95
Re_2**5**	0.215	0.035	0.035	0.215	0.500	−8.77	−3.41	1.89
Re_2**6**	0.213	0.035	0.035	0.213	0.497	−8.73	−3.32	1.95
Re_2**7**	0.191	0.042	0.042	0.191	0.467	−8.85	−3.59	1.86
Re_2**8**	0.212	0.033	0.033	0.212	0.491	−8.78	−3.48	1.85

Table 3 Electronic absorption bands of **1**–**8** and their {$Re(CO)_3Cl$} complexes measured in CH_2Cl_2 at various concentrations

	λ/nm (ε/10^3 dm^3 mol^{-1} cm^{-1})							
	π–π*	π–π*	π–π*	π–π*				
1[a]	255 (89)	334 (27)						
2[a]	261 (87)	324 (26)						
3	284 (87)	319 (73)	354 (sh) (25)	382 (20)				
4[a]	260 (88)	349 (24)						
5	264 (62)	336 (36)						
6	270 (56)	340 (36)						
7	262 (74)	334 (72)						
8	267 (69)	340 (33)						
	π–π*	π–π*		MLCT	MLCT		MLCT	
Re**1**	273 (34)	320 (17)	393 (14)				458 (4.1)	
Re**2**	277 (43)	325 (29)	391 (sh) (21)	405 (22)			448 (sh) (4.8)	
Re**3**	293 (37)	328 (33)	352 (31)	402 (15)	420 (17)		465 (5.2)	
Re**4**	275 (43)	325 (24)	390 (17)	410 (19)			480 (3.7)	
Re**5**	279 (37)	332 (28)		403 (19)			494 (3.8)	
Re**6**	266 (45)	283 (sh) (41)	334 (35)	402 (sh) (24)	420 (25)		477 (4.7)	
Re**7**	272 (51)	348 (48)			420 (sh) (21)		505 (5.5)	
Re**8**	285 (46)	335 (34)			424 (24)		508 (4.1)	
	π–π*		π–π*	MLCT	MLCT		MLCT	MLCT
Re_2**1**	244 (41)	288 (31)	360 (27)	384 (sh) (23)	422 (sh) (20)		511 (7.9)	615 (sh) (3.4)
Re_2**2**	247 (43)	292 (28)	366 (30)		416 (25)		476 (sh) (9.8)	598 (sh) (3.4)
Re_2**3**	264 (53)	305 (sh) (30)	368 (36)	410 (38)			523 (9.3)	641 (sh) (4.4)
Re_2**4**	257 (sh) (49)	293 (46)	355 (sh) (32)	364 (35)	438 (30)		532 (10)	637 (sh) (5.2)
Re_2**5**	256 (54)	285 (sh) (34)	384 (38)	406 (38)	430 (sh) (32)		510 (13)	657 (sh) (5.4)
Re_2**6**	266 (43)	303 (sh) (24)	387 (sh) (34)	414 (35)	431 (sh) (33)		489 (sh) (13)	636 (sh) (3)
Re_2**7**	261 (sh) (42)	311 (sh) (28)	392 (38)		433 (45)		530 (10)	666 (sh) (3.5)
Re_2**8**	256 (47)	299 (sh) (30)	383 (33)	408 (33)	428 (31)	451 (35)	522 (11)	672 (sh) (3.6)

[a] Previously published results. See ref. 23.

reproducing the *changes* caused by ligand substitution and the Re centres.

Infrared spectroscopy

The IR spectra of the parent complexes and their reduced counterparts offer a direct probe of the extent of mixing between the ligand π* MO and the dπ MOs of the metal. The wavenumber of these bands are presented in Table 4. The shifts in the ν(C≡O) bands for *fac*-{$Re(CO)_3Cl$} moieties are well documented and the nature of the vibrational modes is quite well understood.[28]

Infrared absorption spectra in the carbonyl region (1850–2100 cm^{-1}) for the {$Re(CO)_3Cl$} complexes of **1**–**8** were measured for both the parent complexes and after photoreduction by triethylamine (Table 4). A set of typical spectral changes is shown in Fig. 3. In the spectra of the parent complexes the lowest energy band, ν_A, was in the range 1904–1926 cm^{-1}. The next band, ν_B, was in the range 1928–1953 cm^{-1} and the higher energy band, ν_C, was in the range 2022–2027 cm^{-1}. For the binuclear complexes, a shoulder is also observed in the range 2030–2037 cm^{-1}. These data are consistent with other *fac*-{$Re(CO)_3Cl$} complexes.[29,30]

For the mononuclear complexes, the three band pattern of one high wavenumber mode and two lower wavenumber modes, close together, are reproduced from the PM3 frequency calculation. It is possible to invoke scaling factors to better match the predicted frequencies to experimental values,[31] however, our interest lies in a qualitative understanding of this spectral region and how substitution alters this region. We therefore use the unscaled computational outputs.

The mononuclear complexes all show three bands in their experimental infrared spectra in the CO region. The general form of the predicted wavenumbers correlate well with those

Table 4 Infrared absorption data for {$Re(CO)_3Cl$} complexes of **1**–**8** in CH_2Cl_2 (ground state) and CH_2Cl_2–Et_3N (4 : 1) for the photoreduced complexes. Typically 1 mM solutions were used depending on solubility. Band positions were estimated as gaussian functions using curve fitting software

	ν/cm^{-1}							ν/cm^{-1}			
Compound	Experimental			Calculated			k_{CO}[b]/N m^{-1}	Reduced species			Δk[c]/N m^{-1}
Re(bpy)[a]	1899	1917	2023	1922	1960	2123	1531	1867	1881	1996	49
Re**1**	1905	1931	2024	1921	1956	2119	1542	1871	1895	2003	47
Re**2**	1904	1928	2023	1921	1954	2118	1539	1869	1894	2002	46
Re**3**	1905	1929	2023	1922	1955	2118	1540		n.d.[d]		n.d
Re**4**	1909	1935	2027	1922	1958	2119	1548	1878	1893	2007	48
Re**5**	1911	1936	2026	1931	1951	2119	1548		n.d		n.d.
Re**6**	1909	1933	2025	1930	1950	2119	1545	1881	1906	2006	38
Re**7**	1911	1936	2025	1932	1950	2118	1548	1881	1903	2007	43
Re**8**	1914	1939	2027	1931	1953	2119	1552	1885	1908	2009	41
Re_2**1**	1915	1940	2023	1924	1925	1965	1553	1895	1912	2009	33
			2032	1967	2114	2123				2017	
Re_2**2**	1913	1937	2023	1923	1925	1962	1550	1892	1909	2008	33
			2031	1965	2114	2122				2018	
Re_2**3**	1914	1938	2022	1924	1926	1963	1550	1895	1910	2009	30
			2030	1966	2113	2122				2022	
Re_2**4**	1918	1943	2024	1924	1926	1966	1557	1895	1914	2010	35
			2033	1969	2114	2122				2020	
Re_2**5**	1921	1950	2027	1932	1934	1958	1563	1900	1917	2009	38
			2037	1962	2114	2123				2020	
Re_2**6**	1922	1946	2026	1931	1933	1955	1561	1900	1916	2008	36
			2035	1958	2114	2122				2019	
Re_2**7**	1920	1950	2025	1933	1935	1968	1562	1897	1921	2010	34
			2036	1971	2112	2121				2025	
Re_2**8**	1926	1953	2027	1932	1934	1959	1568	1901	1921	2011	39
			2037	1962	2114	2122				2020	

[a] Data measured in CH_3CN; taken from ref. 29. [b] $k_{CO} = (k_{ax} + 2k_{eq})/3$. [c] $\Delta k = k_{CO}$(parent species) $- k_{CO}$(reduced species). [d] n.d. = No data available.

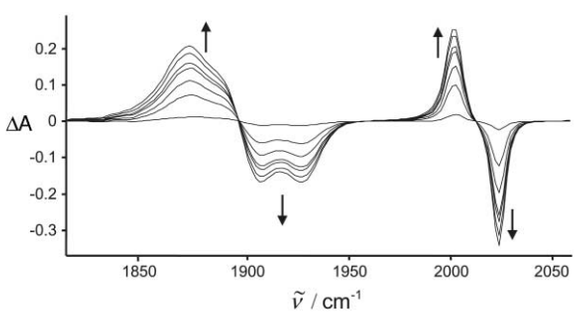

Fig. 3 Infrared difference spectrum for Re**5** in CH_2Cl_2 undergoing photoreduction. Arrows depict the spectral changes as reduction occurs.

observed. A higher wavenumber band is predicted at 2119 cm^{-1}; one is observed at about 2025 ± 2 cm^{-1}. This band is predicted to remain constant throughout the series of mononuclear complexes and this is observed. The calculation also provides a normal mode associated with this transition. This is the symmetric stretch of all three CO bonds, with an in phase motion of the CO_{axial} (internal coordinate r_1) and two $CO_{equatorial}$ (internal coordinates r_2 and r_3) bonds. The details of the labelling are shown on Fig. 2. The mode is described qualitatively as $r_1 + r_2 + r_3$.[32] At lower wavenumbers two bands are predicted about 20 cm^{-1} apart. The experimental data show two bands that vary in separation by *ca.* 15–25 cm^{-1}. These bands show a pattern with respect to ligand substitution. The dqq complexes (Re**1**–Re**4**) show a lower wavenumber for ν_A (1905–1909 cm^{-1}) than complexes with dqxq ligands (Re**5**–Re**8**). The predicted wavenumber is 1921 cm^{-1} for the dqq series and 1931 cm^{-1} for the dqxq series. In all cases this corresponds to a mode described as $2r_1 - r_2 - r_3$. The intermediate wavenumber band (ν_B) is predicted to have a higher wavenumber for the dqq series than dqxq; this prediction poorly reflects the experimental data. The normal mode associated with ν_B is $r_2 - r_3$. These modes are related to those reported for {$Re(CO)_3Cl$} fragments by Turner and coworkers.[33]

The binuclear complexes show four bands in the CO region. Calculations predict six CO bands, however, in the lower wavenumber region the splitting between bands is of the order of 2 cm^{-1} and only the higher wavenumber mode shows appreciable splitting. The form of the normal modes from the calculations may be analysed and this reveals that the highest wavenumber mode ($\nu_{A'}$) is $r_1 + r_2 + r_3 + r_4 + r_5 + r_6$, that is the in-phase ν_A of each {$Re(CO)_3Cl$} unit. The next mode predicted ($\nu_{A''}$) is $r_1 + r_2 + r_3 - r_4 - r_5 - r_6$. This is the out-of-phase symmetric stretch of each {$Re(CO)_3Cl$} unit. The internal coordinates for the CO ligands are given in Fig. 2. The predicted splitting is 8 cm^{-1} and 8 ± 2 cm^{-1} is observed. The next two bands ($\nu_{B'}$ and $\nu_{B''}$) are predicted to lie within 3 cm^{-1} of each other, they are described by: $r_2 - r_3 + r_6 - r_5$ and $r_3 - r_2 + r_5 - r_6$, respectively. The lowest two bands ($\nu_{C'}$ and $\nu_{C''}$), predicted to lie within 2 cm^{-1} of each other are described by: $r_2 + r_3 - 2r_1 + 2r_4 - r_5 - r_6$ and $2r_1 - r_2 - r_3 - 2r_4 + r_5 + r_6$ respectively. The experimental difference between ν_C and ν_B for Re_2**1**–Re_2**8** are about 20 cm^{-1}. The calculations predict a larger splitting, approximately 30–40 cm^{-1}.

The shifts in the ν(C≡O) on going from the ground to MLCT excited state of [$Re(CO)_3Cl$(bpy)] have been measured.[34] Previous studies using time-resolved resonance Raman spectroscopy suggest that the charge-transfer for the MLCT state is about +0.8 charge on the metal and this leads to the shifts to higher wavenumber for the CO bands.[35,36] The shifts in wavenumber of bands alone are not fully informative as to the bonding changes that are occurring about the Re centre. A more insightful approach is to determine the force constants of the normal modes of vibration associated with the CO ligands, to give the k_{ax} and k_{eq} force constants (ax refers to C≡O ligands *trans* to Cl, eq refers to C≡O ligands *cis* to Cl). Using these infrared data it is possible to calculate force constants for the axial (k_{ax}) and equatorial (k_{eq}) carbonyl bonds along with interaction constants for local interactions at a metal centre (k_l). In the case of the binuclear complexes an additional interaction constant is invoked (k_b) that represents the interaction of equatorial CO ligands on adjacent metal sites. The average carbonyl force constant (k_{CO}) is given by $k_{CO} = (k_{ax} + 2k_{eq})/3$.

Results for the complexes along with the changes upon photoreduction are given in Table 4 and Table S1 (ESI†. The force constant calculations followed the approach of Braterman,[37] Cotton[38] and Turner.[39]

The average change in the carbonyl force constants with reduction (Δk)[40] is a consequence of the dπ–π*(L) back-bonding. This interaction produces a delocalised LUMO which is predominantly a pure ligand π* MO with a smaller percentage of (dπ + π^*_{CO}) character contributed from the molecular orbitals of the {$Re(CO)_3Cl$} moiety. Occupation of the LUMO by photoreduction results in the population of the π^*_{CO} MO and hence the bonding changes ($\Delta k < 0$) as observed. The percentage of (dπ + π^*_{CO}) character in the LUMO is related to the amplitude of the π*(L) MO at the chelating N atoms and the difference in energy between the respective MOs. The amplitude of the π*(L) wavefunction may be obtained from the PM3 calculations and is parameterised by Σc_N^2 (Table 2)while the energy between the respective dπ and π*(L) MOs is provided by the electronic spectral data. A plot (Fig. 4) of Δk *vs*

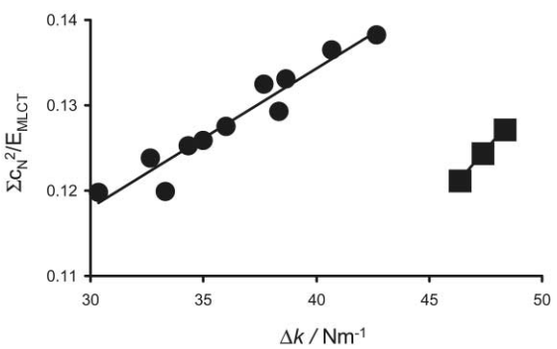

Fig. 4 Plot of Δk *vs.* $\Sigma c_N^2/E_{MLCT}$ for mononuclear complexes Re**1**, Re**2** and Re**4** (■) and complexes Re**5**–Re_2**8** (●)

$\Sigma c_N^2/E_{MLCT}$ is linear ($\Delta k = 0.0016\Sigma c_N^2/E_{MLCT} + 0.069$) for most of the complexes studied herein (Re**5**–Re_2**8**). The remaining complexes (Re**1**, Re**2** and Re**4**) also show a linear relationship between Δk and $\Sigma c_N^2/E_{MLCT}$ ($\Delta k = 0.0030\Sigma c_N^2/E_{MLCT} - 0.017$) but the slope and intercept for these complexes differs significantly from that of the others.[41] The fact that the mononuclear Re–dqq complexes (Re**1**–Re**4**) appear to be much more sensitive to substitution of the quinoxaline bridge ring substitution may be a consequence of the polarisation of the π* MO towards the bridging ring.

The shifts of the observed k_{CO} with reduction suggest that for many of these complexes there is significant electron density of the redox MO on the metal site. Studies of the excited state infrared spectra of [$ReCl(CO)_3$(4,4′-bpy)$_2$] show a Δk of about 80 N m^{-1}.[44] The excited state probed is formally a MLCT state where the oxidation number of the metal is altered by +1. This Δk can be related to changes in the bond length of the CO ligands (r_{CO}) through an adaptation of Badger's rule,[42,43] where $r_{CO} = 1.647–0.184\ln(k_{CO})$.[44] For the excited state of [$ReCl(CO)_3$(4,4′-bpy)$_2$] the change in CO ligand bond length from ground state (Δr_{CO}) is of the order of −0.010 Å. For the complexes studied herein the change in CO bond length on going from the parent species to the reduced species (Δr_{CO}) corresponds to: +0.007 Å for Re**1**, Re**2** and Re**4**; +0.006 Å for Re**6**–Re**8** and between +0.004 and +0.005 Å for the binuclear complexes. These changes suggest sizeable components of the redox MO lie on the metal site. If we assume the force constant changes are directly related to bond order, which in turn relates to the charge at the Re centre then for the Re–dqq complexes the charge leakage on to the Re must be of the order of −0.5 to cause the Δk observed. The binuclear complexes are remarkable in that the charge leakage is close to −0.3 per Re site; this means the majority of the redox MO is in fact metal-based.

Conclusions

A series of rhenium(I) complexes with bridging polypyridyl ligands have been synthesised. The nature of the electron accepting π* MO has been investigated by analysis of the electrochemical, UV–Vis and IR data. The perturbation of the π* MO for the BL appears to be critically controlled by the presence of the Re(I) centre. It is found that substituents on the bridging quinoxaline moiety make very little difference to the bonding/energetic properties of the complexes. The data from this study suggests the redox MO for metal complexes may possess significant dπ character in a formal π* ligand MO; particularly for binuclear complexes in which the energy differences between dπ HOMO and π* LUMO are smaller.

We have also shown that semi-empirical calculations can provide useful insight into the electronic and vibrational properties of large polyatomic metal complexes.

Experimental

Synthesis

1,2-(2′,2″)-Diquinolylethenediol. Quinoline 2-carbaldehyde was purchased from Aldrich and used without further purification. A benzoin condensation[45] was employed to produce the product. In a typical preparation quinoline 2-carbaldehyde (2.5 g, 16 mmol) was refluxed in ethanol (20 mL). While stirring, NaCN (0.14 g, 2.9 mmol) was added, and the mixture was refluxed for 10 min. A red–brown solid was collected by filtration while the mixture was still hot. The filtrate was then brought to reflux again at which point more quinoline 2-carbaldehyde could be added. The solid product was washed with cold water and dried under vacuum. Yield: (1.7 g, 69%). ^{1}H NMR ($CDCl_3$): δ 7.534 (dd, J = 6.6, 6.9 Hz, 2H, 6′, 6″); 7.734 (dd, J = 6.9, 6.9 Hz, 2H, 7, 7″); 7.833 (d, J = 8.1 Hz, 2H, 5′, 5″); 8.014 (d, J = 7.5 Hz, 2H, 8′, 8″); 8.133 (d, J = 8.7 Hz, 2H, 3′, 3″); 8.293 (d, J = 8.7 Hz, 2H, 4′, 4″).

2,2′-Quinadil: (1,2-(2′,2″)-diquinolylethanedione). 2,2′-Quinadil was prepared by literature methods.[45]

Quinoxaline 2-carbaldehyde. Quinoxaline 2-carbaldehyde was prepared by modifying the procedure of Kaplan.[46] 2-Methylquinoxaline was purchased from Aldrich and used without further purification. Selenium dioxide (11.5 g, 104 mmol) was added to a mixture of *p*-dioxane (120 mL) and H_2O (5 mL) and heated to reflux. 2-Methylquinoxaline (10 g, 69 mmol) was dissolved in *p*-dioxane (20 mL) and added dropwise to the refluxing solution. A colour change to red–brown was observed. After refluxing for 4 hours the hot mixture was filtered through Celite and washed with *p*-dioxane (2 × 50 mL). The filtrate was allowed to cool. The wet red–brown solid was extracted into hexane (500 mL) using a Soxhlet apparatus over a period of 24 hours. After cooling the orange hexane solution was dried under vacuum and the product was recrystallised from CH_3OH–H_2O. Yield: (8.0 g, 73%). ^{1}H NMR ($CDCl_3$): δ 7.930 (m, 2H, 6, 7); 8.219 (d, J = 8.1 Hz, 1H, 5); 8.265 (d, J = 7.3 Hz, 1H, 8); 9.437 (s, 1H, 3); 10.270 (s, 1H, CHO). Anal. Calc. for $C_9H_6N_2O$: C, 68.35; H, 3.82; N, 17.71. Found: C, 68.28; H, 3.95; N, 17.85.

1,2-(2′,2″)-Diquinoxalylethenediol. 1,2-(2′,2″)-Diquinoxalylethenediol was prepared, in an analogous fashion to 1,2-(2′,2″)-diquinolylethenediol by replacing quinoline 2-carbaldehyde with quinoxaline 2-carbaldehyde (2.0 g, 13 mmol). The product was isolated as a red solid. Yield: (1.2 g, 61%). ^{1}H NMR ($CDCl_3$): δ 7.801 (m, 4H, 6′, 6″, 7′, 7″); 8.026 (dd, J = 7.4, 2 Hz, 2H, 5′, 5″); 8.151 (dd, J = 7.2, 1.8 Hz, 2H, 8′, 8″); 9.566 (s, 1H, 3′, 3″).

2,2′-Quinoxadil (1,2-(2′,2″)-diquinoxalylethanedione). 2,2′-Quinoxadil was prepared in an analogous fashion to 2,2′-quinadil by replacing to 1,2-(2′,2″)-diquinolylethenediol with 1,2-(2′,2″)-diquinoxalylethenediol (1.0 g, 3.2 mmol). The product was isolated as an orange solid. Yield: (0.54 g, 54%). ^{1}H NMR ($CDCl_3$): δ 7.772 (dd, J = 7.0, 6.9 Hz, 2H, 7′, 7″); 7.914 (dd, J = 8.3, 7.0 Hz, 2H, 6′, 6″); 7.966 (d, J = 8.5 Hz, 2H, 5′, 5″); 8.221 (d, J = 8.8 Hz, 2H, 8′, 8″); 9.705 (s, 2H, 3′, 3″).

Pentacarbonylchlororhenium(I). Pentacarbonylchlororhenium(I) was prepared using literature methods.[47]

Ligands. Ligands were prepared by the Schiff base condensation of a 1,2-diaminobenzene derivative and 2,2′-quinadil or 2,2′-quinoxadil.[48] 1,2-diaminobenzene, 4,5-dimethyl-1,2-diaminobenzene, 4,5-dichloro-1,2-diaminobenzene, and 2,3-diaminonapthalene were all purchased from Aldrich and used without further purification. In a typical preparation 2,2′-quinadil (0.3 g, 1.0 mmol) and the appropriate diaminobenzene (1.0 mmol) were suspended in ethanol (100 mL, freshly distilled from Mg/I_2)[49] and refluxed for one hour. An orange–yellow colour change was observed in the solution phase. After cooling, the solvent was removed under vacuum and the ligand was recrystallised from ethanol–H_2O.

The synthesis of 2,3-(2′,2″)-diquinolylquinoxaline (**1**), 6,7-dimethyl-2,3-(2′,2″)-diquinolylquinoxaline (**2**) and 6,7-dichloro-2,3-(2′,2″)-diquinolylquinoxaline (**4**) has been previously described.[23]

*2,3-(2′,2″)-Diquinolylbenzoquinoxaline (**3**).* The product was isolated as a light brown solid. Yield: 0.2 g, 63%. ^{1}H NMR ($CDCl_3$): δ 7.499 (m, 6H, 5′, 5″, 6′, 6″, 7′, 7″); 7.619 (dd, J = 6.6, 3 Hz, 2H, 7, 8); 7.813 (dd, J = 6.6, 2.7 Hz, 2H, 8′, 8″); 8.170 (dd, J = 6.3, 3.3 Hz, 2H, 6, 9); 8.215 (d, J = 8.7 Hz, 2H, 3′, 3″); 8.285 (d, J = 8.8 Hz, 2H, 4′, 4″); 8.865 (s, 2H, 5, 10). ^{13}C NMR ($CDCl_3$): (15 signals) δ 121.61, 126.88, 127.08, 127.38, 127.44, 128.06, 128.71, 129.40, 129.40, 134.44, 136.32, 137.73, 147.19, 153.26, 157.32. Anal. Calc. for $C_{30}H_{18}N_4$: C, 82.9; H, 4.2; N, 12.9. Found: C, 83.2; H, 4.0; N, 13.0%.

*2,3-(2′,2″)-Diquinoxalylquinoxaline (**5**).* The product was isolated as a orange–brown solid. Yield: 0.4 g, 86%. ^{1}H NMR ($CDCl_3$): δ 7.539 (d, J = 8.4 Hz, 2H, 5′, 5″); 7.624 (dd, 8.4, 6.7 Hz, 2H, 6′, 6″); 7.750 (dd, J = 6.7, 6.7 Hz, 2H, 7′, 7″); 7.949 (dd, J = 6.5, 3.5 Hz, 2H, 6, 7); 8.153 (d, J = 8.1 Hz, 2H, 8′, 8″); 8.345 (dd, J = 6.4, 3.5 Hz, 2H, 5, 8); 9.643 (s, 2H, 3′ 3″). ^{13}C NMR ($CDCl_3$): (12 signals) δ 129.15, 129.37, 129.72, 130.24, 130.51, 131.61, 140.92, 141.35, 141.70, 145.77, 150.18, 151.35. Anal. Calc. for $C_{24}H_{14}N_6$: C, 74.59; H, 3.65; N, 21.75. Found: C, 74.55; H, 3.56; N, 21.84.

*6,7-Dimethyl-2,3-(2′,2″)-diquinoxalylquinoxaline (**6**).* The product was isolated as light pink solid. Yield: 0.5 g, 85%. ^{1}H NMR ($CDCl_3$): δ 2.599 (s, 6H, –C**H**$_3$); 7.532 (dd, J = 8.3, 6.6 Hz, 2H, 6′, 6″); 7.616 (d, J = 8.1 Hz, 2H, 5′, 5″); 7.735 (dd, J = 6.5, 6.7 Hz, 7′, 7″); 8.080 (s, 2H, 5, 8); 8.140 (d, J = 8.1 Hz, 2H, 8′, 8″); 9.609 (s, 2H, 3′, 3″). ^{13}C-NMR ($CDCl_3$): (13 signals) δ 20.56, 128.55, 129.04, 129.26, 130.03, 130.22, 140.28, 140.87, 141.53, 142.51, 145.83, 149.10, 151.56. Anal. Calc. for $C_{26}H_{18}N_6$: C, 75.34; H, 4.38; N, 20.28. Found: C, 75.15; H, 4.34; N, 20.43%.

*2,3-(2′,2″)-Diquinoxalylbenzoquinoxaline (**7**).* The product precipitated directly out of the reaction mixture as a bright yellow solid. Yield: 0.4 g, 63%. ^{1}H NMR ($CDCl_3$): δ 7.494 (d, J = 8.4 Hz, 2H. 5′, 5″); 7.599 (dd, J = 8.5, 6. 8 Hz, 2H, 6′, 6″); 7.675 (dd, J = 6.5, 3.3 Hz, 2H, 7, 8); 7.747 (dd, J = 6.8, 6.7 Hz, 2H, 7′, 7″); 8.167 (d, J = 9 Hz, 2H, 8′, 8″); 8.215 (dd, J = 6.3, 3.3 Hz, 2H, 6, 9); 8.921 (s, 2H, 5, 10); 9.720 (s, 2H, 3′, 3″). ^{13}C NMR ($CDCl_3$): (14 signals) δ 127.73, 128.56, 128.89, 129.21, 129.37, 130.30, 130.57, 134.97, 137.60, 140.90, 141.80, 145.83, 150.65, 151.46. Anal. Calc. for $C_{28}H_{16}N_6$: C, 77.05; H, 3.70; N, 19.26. Found: C, 76.83; H, 3.69; N, 19.16%.

*6,7-Dichloro-2,3-(2′,2″)-diquinoxalylquinoxaline (**8**).* The product precipitated directly out of the reaction mixture as a cream solid. Yield: 0.3 g, 58%. ^{1}H NMR ($CDCl_3$): δ 7.488 (d, J = 8.4 Hz, 2H, 5′, 5″); 7.608 (dd, J = 8.4, 6.8 Hz, 2H, 6′, 6″); 7.760 (dd, J = 6.8, 6.8 Hz, 2H, 8′, 8″); 8.159 (d, J = 8.1 Hz, 2H, 8′, 8″); 8.464 (s, 2H, 5, 8); 9.615 (s, 2H, 3′, 3″). ^{13}C NMR ($CDCl_3$): (12 signals) δ 129.23, 129.36, 130.24, 130.43, 130.81, 136.48, 139.98, 140.85, 141.84, 145.54, 150.72, 151.27. Anal. Calc. for $C_{24}H_{12}N_6Cl_2$: C, 63.31; H, 2.66; N, 18.46. Found: C, 63.35; H, 2.61; N, 18.54%.

Rhenium(I) complexes. Tricarbonylchlororhenium(I) complexes were prepared using established literature methods.[50] If purification was necessary the crude product was dissolved in CH_2Cl_2 (~200 mL) and then chromatographed using a silica column. The binuclear complex was eluted first with CH_2Cl_2; the mononuclear complex was then eluted with CH_3CN.

*Cl(CO)$_3$Re(**1**) (Re**1**).* Re**1** was isolated as an orange solid. Yield: 0.2 g, 65%. Anal. Calc. for $C_{29}H_{16}N_4O_3ClRe$: C, 50.47; H, 2.34; N, 8.12. Found: C, 50.08; H, 2.26; N, 8.24%.

*Cl(CO)$_3$Re(**2**) (Re**2**).* Re**2** was isolated as a light-orange solid. Yield: 0.1 g, 71%. Anal. Calc. for $C_{31}H_{20}N_4O_3ClRe$: C, 51.84; H, 2.81; N, 7.80. Found: C, 51.71; H, 2.78; N, 7.78%.

*Cl(CO)$_3$Re(**3**) (Re**3**).* Re**3** was isolated as an orange solid. Yield: 0.15 g, 76%. Anal. Calc. for $C_{33}H_{18}N_4O_3ClRe(CH_3OH)$: C, 52.90; H, 2.87; N, 7.26. Found: C, 52.74; H, 2.60; N, 7.37%.

*Cl(CO)$_3$Re(**4**) (Re**4**).* Re**4** was isolated as an orange solid. Yield: 0.11 g, 69%. Anal. Calc. for $C_{29}H_{14}N_4Cl_3O_3Re$: C, 45.89; H, 1.86; N, 7.38. Found: C, 46.21; H, 1.82; N, 7.61%.

*Cl(CO)$_3$Re(**5**) (Re**5**).* Re**5** was isolated as a light-red solid. Yield: 0.14 g, 81%. Anal. Calc. for $C_{27}H_{14}N_6O_3ClRe$: C, 46.85; H, 2.04; N, 12.15. Found: C, 46.94; H, 1.85; N, 12.30%.

*Cl(CO)$_3$Re(**6**) (Re**6**).* Re**6** was isolated as a red solid. Yield: 0.1 g, 63%. ^{1}H NMR ($CDCl_3$): δ 2.639 (s, 3H, –CH_3(7)); 2.704 (s, 3H, –CH_3(6)); 7.815 (dd, J = 6.8, 6.8 Hz, 1H, 6′); 7.911 (dd, J = 6.8, 6.8 Hz, 1H, 7′); 7.980 (d, J = 7.1 Hz, 1H, 5′); 7.992 (dd, J = 6.6, 7 Hz, 1H, 6″); 8.083 (dd, J = 6.8, 7 Hz, 1H, 7′); 8.112 (d, J = 6.8 Hz, 1H, 5″); 8.163 (s, 1H, 8); 8.254 (d, J = 7.3 Hz, 1H, 8′); 8.590 (s, 1H, 5); 8.777 (s, 1H, 3″) 8.929 (d, 7.8 Hz, 1H, 8″); 9.853 (s, 1H, 3′). Anal. Calc. for $C_{29}H_{18}N_6O_3ClRe$: C, 48.36; H, 2.52; N, 11.67. Found: C, 48.45; H, 2.42; N, 11.84%.

*Cl(CO)$_3$Re(**7**) (Re**7**).* Re**7** was isolated as a dark-red solid. Yield: 0.11 g, 61%. Anal. Calc. for $C_{31}H_{16}N_6O_3ClRe$: C, 50.17; H, 2.17; N, 11.33. Found: C, 50.30; H, 2.02; N, 11.46%.

*Cl(CO)$_3$Re(**8**) (Re**8**).* Re**8** was isolated as a dark-red solid. Yield: 0.1 g, 65%. Anal. Calc. for $C_{27}H_{12}N_6Cl_3O_3Re$: C, 42.61; H, 1.59; N, 11.04. Found: C, 42.82; H, 1.30; N, 11.17%.

The preparations of binuclear {$Re(CO)_3Cl$} complexes followed the method previously reported.[14] Compound purification was achieved with column chromatography (silica, eluent 4 : 1 CH_2Cl_2–hexane solution).

*Cl(CO)$_3$Re(μ-**1**)Re(CO)$_3$Cl (Re$_2$**1**).* Re$_2$**1** was isolated as a dark-purple solid. Yield: 0.1 g, 60%. ^{1}H NMR ($CDCl_3$): δ 7.882 (dd, J = 7.1, 7.1 Hz, 2H, 6′, 6″); 7.988 (d, J = 7.4 Hz, 2H, 5′, 5″); 8.112 (ddd, J = 6.8, 6.8, 1.7 Hz, 2H, 7′, 7″); 8.173 (dd, J = 6.6, 3.4 Hz, 2H, 6, 7); 8.377 (d, J = 8.8 Hz, 2H, 8′, 8″); 8.732 (6.6, 3.4 Hz, 2H, 5, 8); 8.773 (d, J = 8.8 Hz, 2H, 4′, 4″); 8.942 (d, J = 9 Hz, 2H, 3′, 3″). Anal. Calc. for $C_{32}H_{16}N_4O_6Cl_2Re_2$: C, 38.59; H, 1.62; N, 5.63. Found: C, 38.45; H, 1.74; N, 5.54%.

*Cl(CO)$_3$Re(μ-**2**)Re(CO)$_3$Cl (Re$_2$**2**).* Re$_2$**2** was isolated as a dark-red solid. Yield: 0.07 g, 48%. ^{1}H NMR ($CDCl_3$): δ 2.686 (s, 6H, –CH_3); 7.856 (dd, J = 7.1, 6.7 Hz, 2H, 6′, 6″); 7.9682 (dd, J = 8.1, 1.5 Hz, 2H, 5′, 5″); 8.094 (ddd, J = 6.9, 6.7, 1.8 Hz, 2H, 7′, 7″); 8.331 (d, J = 8.4 Hz, 2H, 8′, 8″); 8.464 (s, 2H, 5, 8); 8.683 (d, J = 8.7 Hz, 2H, 4′, 4″); 8.953 (d, J = 8.8 Hz, 2H, 3′, 3″). Anal. Calc. for $C_{34}H_{20}N_4O_6Cl_2Re_2$: C, 39.89; H, 1.97; N, 5.47. Found: C, 39.76; H, 1.79; N, 5.72%.

*Cl(CO)$_3$Re(μ-**3**)Re(CO)$_3$Cl (Re$_2$**3**).* Re$_2$**3** was isolated as a dark-brown solid. Yield: 0.1 g, 75%. Anal. Calc. for $C_{36}H_{18}N_4O_6Cl_2Re_2$: C, 41.34; H, 1.73; N, 5.36. Found: C, 41.63; H, 1.68; N, 5.46%.

*Cl(CO)$_3$Re(μ-**4**)Re(CO)$_3$Cl (Re$_2$**4**).* Re$_2$**4** was isolated as a dark-brown solid. Yield: 0.14 g, 83%. Anal. Calc. for $C_{32}H_{14}N_4Cl_4O_6Re_2$: C, 36.10; H, 1.33; N, 5.6. Found: C, 36.24; H, 1.24; N, 5.33%.

*Cl(CO)$_3$Re(μ-**5**)Re(CO)$_3$Cl (Re$_2$**5**).* Re$_2$**5** was isolated as a dark-brown solid. Yield: 0.1 g, 67%. Anal. Calc. for $C_{30}H_{14}N_6O_6Cl_2Re_2 \cdot 0.25CH_2Cl_2$: C, 35.65; H, 1.43; N, 8.25. Found: C, 35.55; H, 1.20; N, 7.86%.

*Cl(CO)$_3$Re(μ-**6**)Re(CO)$_3$Cl (Re$_2$**6**).* Re$_2$**6** was isolated as a black solid. Yield: 0.04 g, 34%. ^{1}H NMR ($CDCl_3$): δ 2.707 (s, 6H, –CH_3); 8.114 (m, 4H, 6′, 6″, 7′, 7″); 8.311 (dd, J = 7.6, 2.2 Hz, 2H, 5′, 5″); 8.424 (s, 2H, 5, 8); 8.819 (d, J = 8.0 Hz, 2H, 8′, 8″); 9.915 (s, 2H, 3′, 3″). Anal. Calc. for $C_{32}H_{18}N_6O_6Cl_2Re_2$: C, 37.47; H, 1.77; N, 8.19. Found: C, 37.77; H, 1.69; N, 8.46%.

Cl(CO)$_3$Re(μ-7)Re(CO)$_3$Cl (Re$_2$7). The preparation of this complex yielded a mixture of the mononuclear and binuclear complexes. Separation could be achieved with column chromatography (silica), however only small amounts of the binuclear complex were recovered. As an alternative, **7** (0.1040 g, 0.24 mmol) was dissolved in N_2 degassed $CHCl_3$, $Re(CO)_5Cl$ (0.2065 g, 0.52 mmol) was added, and the mixture refluxed under N_2 for 7 hours. A colour change to black was observed. The reaction mixture was allowed to cool and the solvent was removed under vacuum. The crude solid was dissolved in CH_2Cl_2, filtered, and the product precipitated by adding Et_2O. The black solid was collected by filtration. Yield: 0.19 g, 70%. Anal. Calc. for $C_{34}H_{16}N_6O_6Cl_2Re_2 0.5CH_2Cl_2$: C, 38.01; H, 1.58; N, 7.71. Found: C, 37.76; H, 1.75; N, 7.23%.

*Cl(CO)$_3$Re(μ-**8**)Re(CO)$_3$Cl (Re$_2$**8**).* Re$_2$**8** was prepared in an analogous fashion to Re$_2$**7** and was isolated as a black solid. Yield: 0.18 g, 72%. Anal. Calc. for $C_{30}H_{12}N_6Cl_4O_6Re_2$: C, 33.78; H, 1.13; N, 7.88. Found: C, 33.80; H, 1.17; N, 7.69%.

Physical measurements

The instrumentation used in electrochemistry, UV/Vis spectroscopy and spectroelectrochemistry has been detailed elsewhere.[51] Infrared spectra were collected using a BIO–RAD Digilab Division FTS-60 FT-IR with Bio-Rad Win-IR software. Samples were prepared as ~1 mM CH_2Cl_2 solutions. For the reductive quenching experiments, samples were prepared as 1 mM solutions in a freshly prepared mixture of CH_2Cl_2 and NEt_3 (20%).[21] The mononuclear complexes had in addition to this a 0.1 M concentration of Bu_4NCl. The solution was degassed with Ar and a small amount transferred to a solution IR cell. Spectra were measured continuously, while under irradiation from a halogen lamp, with a 4 cm^{-1} resolution for a maximum time of 30 minutes.

Calculations

The force constants of the carbonyl bonds in the binuclear {$Re(CO)_3Cl$} complexes of **1**–**8** were calculated by extending Cotton's approach[38] to a binuclear system under C_2 symmetry. The assignment of the experimental spectra followed the assignment of Turner.[33] An additional interaction between the two carbonyl systems across the bridging ligand was proposed to account for the splitting in energy of the ν_C band. Therefore, four force constants were expected. Each CO stretch was either k_{ax} or k_{eq}; interactions between COs attached to the same rhenium centre were all assumed to be k_l; remote interactions were assumed to be non-zero only for equatorial–equatorial interactions and these were all equal to k_b. It was noted that if $k_b = 0$ then the two centres would be non-interacting and the spectrum should resemble that of a mononuclear system. The system was solved using the linear variation principle from Braterman.[37]

It was also noted that a non-zero value of k_b means that the two ν_B bands do not have equivalent frequencies. However using the calculated k_b value led to a splitting of these bands of *ca.* 2 cm^{-1}. The spectral breadths of these bands suggest they would be difficult to resolve.

PM3 semi-empirical calculations were implemented using the SPARTAN package.[52]

Acknowledgements

Support from the New Zealand Lottery Commission and the University of Otago Research Committee is gratefully acknowledged. A. F. would like to acknowledge the Alliance Group for a post-graduate scholarship.

References

1 F. Scandola, M. T. Indelli, C. Chiorboli and C. A. Bignozzi, *Top. Curr. Chem.*, 1990, **158**, 73; V. Balzani, S. Campagna, G. Denti, A. Juris, S. Serroni and M. Venturi, *Acc. Chem. Res.*, 1998, **31**, 26.
2 H. M. Sung-Suh, D. S. Kim, C. W. Lee and S.-E. Park, *Appl. Organomet. Chem.*, 2000, **14**, 826.
3 M. K. Nazeeruddin, A. Kay, I. Rodicio, R. Humphrey-Baker, E. Mueller, P. Liska, N. Vlachopoulos and M. Gratzel, *J. Am. Chem. Soc.*, 1993, **115**, 6382; K. Kalyanasundaram and M. Gratzel, *Coord. Chem. Rev.*, 1998, **177**, 347; J. E. Moser, P. Bonnote and M. Gratzel, *Coord. Chem. Rev.*, 1998, **177**, 245; C. A. Bignozzi, J. R. Schoonover and F. Scandola, *Prog. Inorg. Chem.*, 1997, **44**, 1.
4 V. Balzani, M. Gomez-Lopez and J. F. Stoddart, *Acc. Chem. Res.*, 1998, **31**, 405; M. Venturi, S. Serroni, A. Juris, S. Campagna and V. Balzani, *Top. Curr. Chem.*, 1998, **197**, 193; R. Ziessel, M. Hissler, A. El-Ghayoury and A. Harriman, *Coord. Chem. Rev.*, 1998, **180**, 1251; R. Ziessel and A. Harriman, *Coord. Chem. Rev.*, 1998, **171**, 331; F. Scandola, R. Argazzi, C. A. Bignozzi, C. Chiorboli, M. T. Indelli, M. A. Rampi, in *Supramolecular Chemistry*, ed. V. Balzani and L. DeCola, Kluwer, Dordrecht, 1992, p. 235.
5 H. Szmacinski and Q. Chang, *Appl. Spectrosc.*, 2000, **54**, 106.
6 C. Turró, Y. C. Chung, N. Leventis, M. E. Kuchenmeister, P. J. Wagner and G. E. Leroi, *Inorg. Chem.*, 1996, **35**, 5104.
7 K. M. Omberg, J. R. Schoonover, S. Berhard, J. A. Moss, J. A. Treadway, E. M. Kober, R. B. Dyer and T. J. Meyer, *Inorg. Chem.*, 1998, **37**, 3505.
8 M. K. DeArmond and M. L. Myrick, *Acc. Chem. Res.*, 1989, **22**, 364.
9 P. G. Bradley, N. Kress, B. A. Hornberger, R. F. Dallinger and W. H. Woodruff, *J. Am. Chem. Soc.*, 1981, **103**, 7441.
10 M. W. George, F. P. A. Johnson, J. R. Westwell, P. M. Hodges and J. J. Turner, *J. Chem. Soc. Dalton Trans.*, 1993, 2977.
11 M. W. George, F. P. A. Johnson, J. J. Turner and J. R. Westwell, *J. Chem. Soc., Dalton Trans.*, 1995, 2711.
12 C. D. Tait, T. M. Vess, M. K. DeArmond, K. W. Hanck and D. W. Wertz, *J. Chem. Soc., Dalton Trans.*, 1987, 2467; R. J. Donohoe, C. D. Tait, M. K. DeArmond and D. W. Wertz, *Spectrochim. Acta, Part A*, 1986, **42**, 233; C. D. Tait, D. B. MacQueen, R. J. Donohoe, M. K. DeArmond, K. W. Hanck and D. W. Wertz, *J. Phys. Chem.*, 1986, **90**, 1766.
13 K. Kalyanasundaram, *Photochemistry of Polypyridine and Porphyrin Complexes*, Academic Press, London, 1992.
14 T. J. Simpson and K. C. Gordon, *Inorg. Chem.*, 1995, **34**, 6323.
15 M. R. Waterland, T. J. Simpson, K. C. Gordon and A. K. Burrell, *J. Chem. Soc., Dalton Trans.*, 1998, 185.
16 W. Kaim and S. Kohlmann, *Inorg. Chem.*, 1990, **29**, 2909.
17 A. Juris, S. Campagna, I. Bidd, J.-M. Lehn and R. Ziessel, *Inorg. Chem.*, 1988, **27**, 4007.
18 L. S. Kelso, D. A. Reitsma and F. R. Keene, *Inorg. Chem.*, 1996, **35**, 5144.
19 J. B. Foresman and A. Frisch, *Exploring Chemsitry with Electronic Structure Methods*, Gaussian Inc., Pittsburgh, 1996.
20 P. Comba and T. W. Hambley, *Molecular Modeling of Inorganic Compounds*, Weinheim, VCH, New York, 1995.
21 V. Enchev, A. Ahmedova, G. Ivanova, I. Wawer, N. Stoyanov and M. Mitewa, *J. Mol. Struct.*, 2001, **595**, 67; B. Rivas, G. V. Seguel and K. E. Geckeler, *J. Appl. Polym. Sci.*, 2001, **81**, 1310; K. H. Lee, Y. S. Suh, S. S. Park, H. P. Luthi and D. H. Kim, *Synth. Met.*, 2001, **121**, 1163; E. Bencze, B. V. Lokshin, J. Mink, W. A. Herrmann and F. E. Kuhn, *J. Organomet. Chem.*, 2001, **627**, 55; A. Acosta, J. I. Zink and J. Cheon, *Inorg. Chem.*, 2000, **39**, 427; E. Akalin and S. Akyuz, *J. Mol. Struct.*, 1999, **482–483**, 175; T. Kupka, *Spectrochim. Acta, Part A*, 1997, **53**, 2649.
22 For *cis*-Re$_2$**1**, the predicted IR spectrum in the CO region has bands at 2125, 2114, 1973, 1960, 1931 and 1926 cm^{-1}.

23 S. E. Page, K. C. Gordon and A. K. Burrell, *Inorg. Chem.*, 1998, **37**, 4452.
24 M. R. Waterland, T. J. Simpson, K. C. Gordon and A. K. Burrell, *J. Chem. Soc., Dalton Trans.*, 1998, 185.
25 W. Kaim and S. Kohlmann, *Inorg. Chem.*, 1987, **26**, 68.
26 J. Sherborne, S. M. Scott and K. C. Gordon, *Inorg. Chim. Acta*, 1997, **260**, 199; J. Sherborne and K. C. Gordon, *Asian J. Spectrosc.*, 1998, **2**, 137.
27 *Inorganic and Electronic Spectorscopy, Volume II, Applications and Case Studies.*, ed. E. I. Soloman and A. B. P. Lever, J. Wiley and Sons Inc., New York, 1999.
28 I. P. Clark, M. W. George and J. J. Turner, *J. Phys. Chem. A.*, 1997, **101**, 8367.
29 I. P. Clark, M. W. George, F. P. A. Johnson and J. J. Turner, *Chem. Commun.*, 1996, 1587.
30 L. C. Abbott, C. J. Arnold, T.-Q. Ye, K. C. Gordon, R. N. Perutz, R. E. Hester and J. N. Moore, *J. Phys. Chem. A.*, 1998, **102**, 1252.
31 S. Schneider, G. Brehm, C. J. Prenzel, W. Jager, M. I. Silva, H. D. Burrows and S. T. Formoshino, *J. Raman Spectrosc.*, 1996, **27**, 163.
32 The exact nature of the normal mode may be established but our qualitative analysis gains little from such an analysis.
33 D. R. Gamelin, M. W. George, P. Glyn, F.-W. Grevels, F. P. A. Johnson, W. Klotzbucher, S. L. Morrison, G. Russell, K. Schaffner and J. J. Turner, *Inorg. Chem.*, 1994, **33**, 3246.
34 I. P. Clark, M. W. George, F. P. A. Johnson and J. J. Turner, *Chem. Commun.*, 1996, 1587.
35 J. V. Caspar, T. D. Westmoreland, G. H. Allen, P. G. Bradley, T. J. Meyer and W. H. Woodruff, *J. Am. Chem. Soc.*, 1984, **106**, 3492.
36 J. I. Zink and K.-S. K. Shin, *Inorg. Chem.*, 1989, **28**, 4358.
37 P. S. Braterman, *Metal Carbonyl Spectra*, Academic Press, London, 1975.
38 F. A. Cotton and C. S. Kraihanzel, *J. Am. Chem. Soc.*, 1962, **84**, 4432.
39 I. P. Clark, M. W. George and J. J. Turner, *J. Phys. Chem. A.*, 1997, **101**, 8367.
40 $\Delta k = \{(k_{ax} + 2k_{eq})_{reduced\ species} - (k_{ax} + 2k_{eq})_{parent\ species}\}/3$ (N m^{-1}).
41 The errors in the gradients of each slope is 1.5×10^{-4} for the Re**5**–Re$_2$**8** data and 1.0×10^{-4} for the Re**1**, Re**2** and Re**4** data.
42 R. M. Badger, *J. Chem. Phys.*, 1934, **2**, 128; R. M. Badger, *Phys. Rev.*, 1935, **48**, 284.
43 V. M. Miskowski, R. F. Dallinger, G. C. Christoph, D. E. Morris, G. H. Spies and W. H. Woodruff, *Inorg. Chem.*, 1987, **26**, 2127; S. D. Conradson, A. P. Sattelberger and W. H. Woodruff, *J. Am. Chem. Soc.*, 1988, **110**, 1309.
44 r_{CO} in Å; k_{CO} in mdyn Å^{-1} S. L. Morrison and J. J. Turner, *J. Mol. Struct.*, 1994, **317**, 39.
45 J. O. Harris and C. A. Buehler, *J. Am. Chem. Soc.*, 1950, **72**, 5015.
46 H. Kaplan, *J. Am. Chem. Soc.*, 1941, **63**, 2654.
47 S. P. Schmidt, W. C. Trogler and F. Basolo, *Inorg. Synth.*, 1990, **28**, 161.
48 H. Goodwin and F. Lions, *J. Am. Chem. Soc.*, 1959, **81**, 6415.
49 D. D. Perrin, W. L. F. Armarego and D. R. Perrin, *Purification of Laboratory Chemicals, 2nd Edn.*, Pergamon Press, Oxford, 1980, p. 552.
50 B. J. Yoblinski, M. Stathis and T. F. Guarr, *Inorg. Chem.*, 1992, **31**, 5.
51 S. M. Scott, A. K. Burrell, P. A. Cocks and K. C. Gordon, *J. Chem. Soc., Dalton Trans.*, 1998, 3679; S. M. Scott, A. K. Burrell and K. C. Gordon, *J. Chem. Soc., Dalton Trans.*, 1998, 2873; S. M. Scott, K. C. Gordon and A. K. Burrell, *Inorg. Chem.*, 1996, **35**, 2452; M. R. Waterland, A. Flood and K. C. Gordon, *J. Chem. Soc., Dalton Trans.*, 2000, 121.
52 PC SPARTAN Pro version 1.0.6, Wavefunction Inc., 18401 Von Karmen Ave., Suite 370, Irvine, CA 92612, USA, 2001.